

RSC Advances



This is an *Accepted Manuscript*, which has been through the Royal Society of Chemistry peer review process and has been accepted for publication.

Accepted Manuscripts are published online shortly after acceptance, before technical editing, formatting and proof reading. Using this free service, authors can make their results available to the community, in citable form, before we publish the edited article. This *Accepted Manuscript* will be replaced by the edited, formatted and paginated article as soon as this is available.

You can find more information about *Accepted Manuscripts* in the [Information for Authors](#).

Please note that technical editing may introduce minor changes to the text and/or graphics, which may alter content. The journal's standard [Terms & Conditions](#) and the [Ethical guidelines](#) still apply. In no event shall the Royal Society of Chemistry be held responsible for any errors or omissions in this *Accepted Manuscript* or any consequences arising from the use of any information it contains.



PAPER

Enhanced thermoelectric properties of PEDOT:PSS films via a novel two-step treatment

Received 00th January 20xx,
Accepted 00th January 20xx

DOI: 10.1039/x0xx00000x

www.rsc.org/

Li Zhang, Hua Deng,* , Siyao Liu, Qin Zhang, Feng Chen, Qiang Fu*

Post-treatment of PEDOT:PSS films to fabricate high performance thermoelectric (TE) materials has been widely studied. The depletion of PSS and tuning the redox level of PEDOT have been considered important. The effective control of these two issues is crucial, yet, not been systematically investigated. Herein, HI and DMSO are used to post-treat PEDOT:PSS films, issues including using these solvents in a step-wise fashion, using solvent or vapour and treatment time are studied. HI is found to have both physical doping and reducing effect on PEDOT:PSS simultaneously. However, HI solution or vapour could not remove most of the excessive PSS to obtain high electrical conductivity. Therefore, DMSO is used firstly to achieve this. Subsequently, HI vapour was used to alter their redox level. Through this method, the power factor reaches as high as 45.02 $\mu\text{W}/\text{mk}^2$, which is over 5000 times higher than the as spun film. These films are characterized with different methods, including: AFM, XPS, UV, SEM and Raman spectroscopy. It is concluded that, such enhancement in TE properties are caused by two issues: the depleting effect of PSS by DMSO and oxidation level change of PEDOT by HI vapour. The former leads to enhanced electrical conductivity and the later leads to reduced charge carrier concentration, thus, enhanced Seebeck coefficient. It is thought that such two-step solvent post-treatment method could offer a novel route to optimize TE properties of PEDOT:PSS based materials.

1. Introduction

Recently, thermoelectric materials that convert waste heat into electricity have attracted much interest as a promising clean-energy technology. It is reported TE properties of various materials can be optimized by controlling their structure in molecular or nano scale¹⁻³, to achieve high thermoelectric conversion efficiency. The performance of TE materials is evaluated by the figure of merit (ZT), which is defined as:

$$ZT = S^2 \sigma T / k \quad (1)$$

where S stands for the Seebeck coefficient (also called the thermopower), σ and k are the electrical conductivity and thermal conductivity, and T is the absolute temperature. $S^2 \sigma$ is also known as the power factor. To achieve high ZT value, materials are required to have a high power factor and low thermal conductivity. However, it is thought that the conflicting relationship between electrical conductivity and Seebeck coefficient limits the further optimization of ZT⁴. Inorganic TE materials have been widely studied due to their high ZT value and high applicable temperature. However, they face several challenges such as toxicity, high-cost, lack of flexibility and high thermal conductivity, leading to the need to explore organic thermoelectric materials.

Organic polymer-based TE materials are eco-friendly, lightweight, low cost, flexible, which draw much attention recently. Compared to inorganic materials, conductive polymers have much lower thermal conductivity, and tunable electrical conductivity^{5, 6}, which could benefit their TE properties⁷. Moreover, conductive polymers can be easily processed and blended with inorganic/organic materials owing to their excellent solubility^{8, 9}. Polypyrrole (PPy)⁸, polyaniline (PANI)^{10, 11}, polycarbazole¹², polythiophene¹³⁻¹⁵ and its ramification^{16, 17} have been widely investigated as TE materials.

Poly(3,4-ethylenedioxythiophene):poly(styrene sulfonate) (PEDOT:PSS) is considered as the most promising conductive polymer for TE application as its electrical conductivity can be enhanced by several orders of magnitude by adding solvent with high dielectric constant^{18, 19}, such as dimethyl sulfoxide (DMSO) and ethylene glycol (EG)^{20, 21}. It is reported that these solvents can orient PEDOT chains, resulting in improvement in charge carriers mobility²². Besides, the power factor can be enhanced by regulating the redox level through chemical or electrochemical method^{23, 24} or altering the physical structure by adding dopant^{25, 26}. The former is able to achieve the optimization of TE properties through the control of charge carrier concentration, while the later through charge carrier mobility. PEDOT can be doped by both inorganic and organic acid²⁷. Xia et al.²⁸ reported that the electrical conductivity of PEDOT:PSS films increases from 0.3 S/cm to 3065 S/cm after PSS being selectively removed with sulfuric acid. As a hydrosoluble inorganic acid, HI is thought to be able to deplete PSS selectively from PEDOT:PSS nanofilms. This could lead to an enhancement in electrical conductivity. Meanwhile, HI could also change the oxidation level of PEDOT as an effective reductant^{29, 30}. A number

College of Polymer Science and Engineering, State Key Laboratory of Polymer Materials Engineering, Sichuan University, Chengdu 610065, China. Fax: 28 8540 5401; Tel: 028 8546 1795; E-mail: huadeng@scu.edu.cn (H. Deng), qiangfu@scu.edu.cn (Q. Fu).
Electronic Supplementary Information (ESI) available. See DOI: 10.1039/x0xx00000x

of studies have demonstrated HI can either selectively remove PSS from PEDOT:PSS³¹ or change their redox level^{20, 32}. Herein, HI solution and vapour is firstly used to post-treat PEDOT:PSS films to optimize their TE properties. It is observed that HI alone could not effectively remove PSS, hence, improve their electrical conductivity. The depletion of insulating PSS from these films as well as the control of the redox level of PEDOT molecular chains are both very important to achieve high performance TE materials. Nevertheless, the simultaneous effective control of these two issues has not been investigated systematically to the best of our knowledge. It is believed that such simultaneous effective control could offer a novel route towards high performance organic TE materials. Therefore, a novel two-step method involves using DMSO firstly to remove PSS, then using HI vapour to alter their redox level, is proposed. The depletion of PSS and redox level of these nanofilms are investigated systematically to correlate with their respective TE properties.

2. Experimental section

2.1 Materials and reagents

PEDOT:PSS aqueous solution (Clevios PH 1000) was purchased from H. C. Stark. The concentration of PEDOT:PSS is 1.3 wt%. The weight ratio of PSS to PEDOT is 2.5. DMSO (99%) and HI (45%) were purchased from Bodi Chemicals (Tianjin, China). All chemicals were used without any further purification.

2.2 Fabrication of PEDOT:PSS films and post-treatment process

Free standing films were treated with HI solution. While PEDOT:PSS nanofilms were spin-coated on a glass substrate as described in our previous report³³. And these nanofilms were treated with two different methods: 1) HI vapour at 100 °C; 2) DMSO at room temperature for 30 min and subsequently HI vapour at 100 °C. Both types of these treated films were immersed in ethanol for 20 min to remove residual solvent and then dried for another 5 min at 130 °C before cooled down to room temperature.

2.3 Characterization

Characterizations including: electrical conductivity, seebeck coefficient, atomic force microscope (AFM), ultraviolet-visible light detector, X-ray photoelectron spectroscopy (XPS), ultraviolet absorption spectra (UV) and Raman spectroscopy were conducted. Electrical conductivity was measured with a four-probe equipment (RTS-8, 4-probes Tech.). The thicknesses (d) of these films were obtained using scanning electronic microscope (SEM) and the accelerating voltage used was 20 KV. Electrical conductivity (s) was calculated as following:

$$S = I / R_s * d \quad (2)$$

Seebeck coefficient was measured by home-made set up at room temperature in ambient atmosphere. Measurements on such set up have been calibrated with nickel alloy samples. These results are also found comparable to the results measured with device from MMR Technologies, Inc. as well as Namicro, GIANT (China). The surface morphology was characterized with AFM (NanoScopeMultiMode Explore, Veeco Instruments) in tapping mode. Absorption spectra of these films were measured using ultraviolet-visible light detector (UV-3600 Shimadzu, Japan). Raman spectra were performed using a 532 nm laser line as an excitation source on Confocal Raman spectrometer (LabRAM HR, HORIBA JobinYvon S.A.S.). X-Ray photoelectron spectroscopy (XPS, Axis Ultra DLD, Kratos Co., UK) characterization was conducted to measure the ratio of PSS and

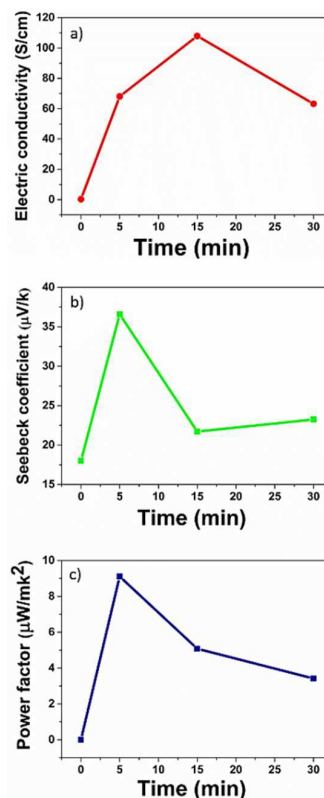


Fig. 1 a) electrical conductivity, b) Seebeck coefficient, c) power factor of PEDOT:PSS nanofilms treated by HI solution

PEDOT on the surface of these films. Freshly made specimens were used for above characterizations.

3. Results and discussion

3.1 HI solution immersing treatment

The electrical conductivity, Seebeck coefficient and power factor of PEDOT:PSS free-standing films as a function of treatment time are measured as shown in Fig.1. The electrical conductivity (shown in Fig1a) increases from 0.3 S/cm to 107.9 S/cm with 15 min treatment, then falls to near 60 S/cm with 30 min treatment. Meanwhile, the Seebeck coefficient (Fig1b) increases from 18 μV/K to as high as 36.59 μV/K with 5 min treatment. The same trend is observed for electrical conductivity. Hence, the power factor (Fig1c) rises to 9.11 μW/mK² with 5 min HI solution treatment, which is over 1000 times higher than that of pristine films (0.008 μW/mK²).

To investigate the mechanism responsible for change in TE properties observed, AFM is used to characterize the surface morphology of PEDOT:PSS nanofilms. These films were transferred topolyethylene terephthalate (PET) film and dried before characterization, since these as-fabricated nanofilms were easily peeled off from substrate after HI solution treatment. It is thought that the morphology observed can be used to indicate the surface morphology of solution treated free-standing films. As shown in Fig.2, it is noted that the surface of these films becomes more rugged, and grain-like morphology is observed after immersion in HI solution. This demonstrates that PSS is efficiently removed from PEDOT:PSS

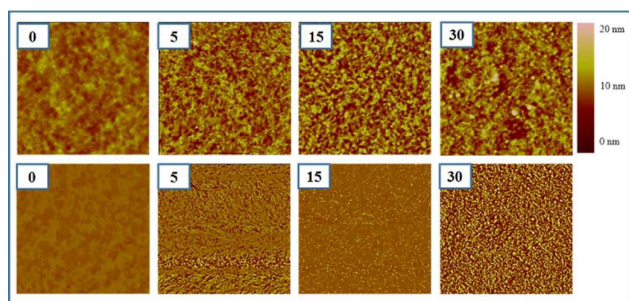


Fig.2 AFM images of PEDOT:PSS nanofilms treated by HI solution for different time, scanning area: $2\ \mu\text{m} \times 2\ \mu\text{m}$

nanofilms. The surface roughness calculated by the height images are 0.888, 1.839, 2.195, 2.08, respectively. The film treated for 15 min has the largest roughness, which might explain the mechanism responsible for the highest electrical conductivity for this particular specimen. In the phase image, bright region corresponding to PEDOT-rich phase, while dark region corresponding to PSS-rich phase. Phase separation is apparently observed after treatment with HI solution, and the degree of phase separation increases over time. This further demonstrates that insulating PSS has been removed from these nanofilms.

To further confirm the selective removal of PSS from these films, the surface chemical compositions were analyzed with XPS. Fig.3(a) shows the XPS spectra of PEDOT:PSS films before and after HI solution treatment. Two characteristic sulfur (S) 2p peaks are detectable in these films. Since the S atoms of thiophene in PEDOT and sulfonate in PSS have different binding energies^{34, 35}, the lower peak (164.6 and 163.4 eV) represents the S atoms in PEDOT while the higher one (169 and 167.8 eV) represents the S atoms in PSS, respectively. Upon treatment, the peak of PSS becomes much weaker, while the peak from PEDOT becomes slightly stronger. Particularly, the ratios between PSS and PEDOT bands area (PSS/PEDOT) were calculated according to these XPS spectra and the formula: $R_{\text{PSS/PEDOT}} = (M_{\text{PEDOT}}/M_{\text{PSS}}) \times r$ ("r" is the ratios of volume between PSS peak and PEDOT peak). As shown in Fig.3(b), the ratio between PEDOT and PSS decreases sharply from 2.312 to 1.225 after 5 min treatment, then keeps decreasing slightly. It demonstrates that PSS could be selectively depleted from these films, which results in an obvious increase in electrical conductivity. It is noted that the ratio of PSS and PEDOT is slightly different from the given value but still within an error range, due to the XPS characterization can only detect elements on the surface of these films, so an exact and thorough reflection of elementary composition is unavailable.

As mentioned above, HI solution has both physical doping and reduction effects, thus, Raman spectra (Fig.4) is used to characterize the redox level of PEDOT:PSS films before and after treatment. Generally, $1425\ \text{cm}^{-1}$ and $1453\ \text{cm}^{-1}$ are assigned to the Raman peaks of symmetric stretching vibration of C α -C β of quinoid and C α =C β of benzoidthiophene ring, respectively.^{36, 37} The main peak for pristine film appears at $1435\ \text{cm}^{-1}$, it is enhanced and became narrower than pristine film, indicating the decrease of doping level from bipolaron to polaron or neutral by HI solution treatment. It is further demonstrated that a dedoping process is occurred to decrease the redox level of PEDOT.

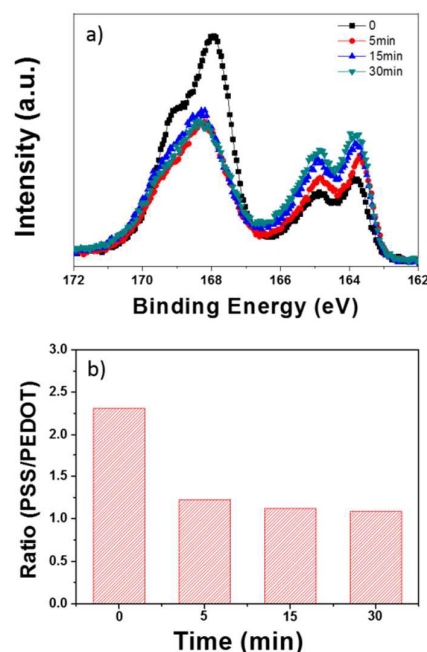


Fig.3 a) pristine XPS spectra (S 2p), b) ratios of PSS and PEDOT

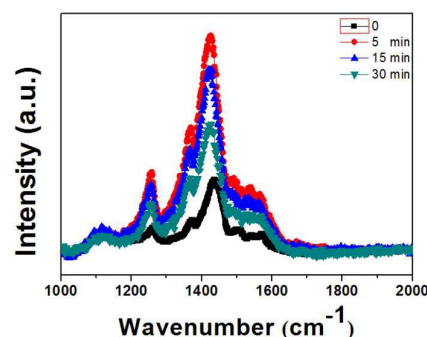


Fig.4 Raman spectra of HI solution treated films

Moreover, the highest intensity is observed when treated for 5 min, which explains the highest value of Seebeck coefficient. Besides, the peak is red shifted from $1435\ \text{cm}^{-1}$ to lower wavenumber ($1425\ \text{cm}^{-1}$), indicating a conformational change of PEDOT chains from coiled benzoid structure to linear quinoid structure^{38, 39}, thus enhances the charge carriers mobility, which is favorable for increase in electrical conductivity.

3.2 HI vapour treatment

It should be noted that the reduction of HI solution is so strong that the highest power factor ($9.11\ \mu\text{W}/\text{mK}^2$) is obtained with only 5 min treatment, and the electrical conductivity starts to decrease after 15 min. This is mainly due to the dynamic balance of physical doping and reduction effect. However, the power factor of these films are still quite low as the HI solution can only remove the PSS and alter the redox level of PEDOT near the film surface. Hence, spin coated films with a thickness in the range of nm is preferred. Nevertheless, as mentioned above, HI solution is found to easily destroy these nanofilms. Therefore, HI vapour is used instead of HI solution to further enhance the TE properties of these nanofilms.

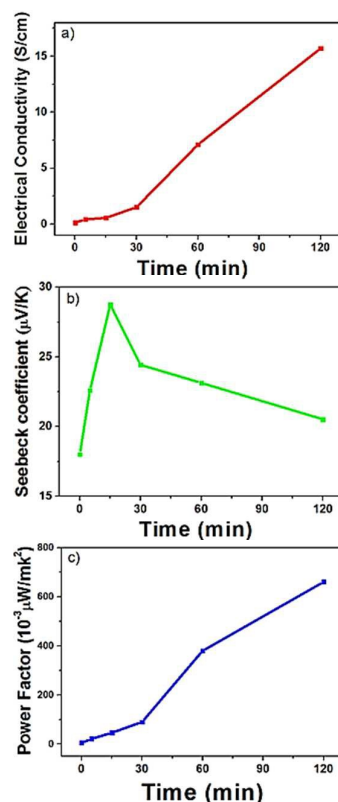


Fig.5 a) electrical conductivity, b) Seebeck coefficient, c) power factor of PEDOT:PSS nanofilms treated by HI vapour.

Fig.5 shows the influence of HI vapour treatment on the TE properties of PEDOT:PSS nanofilms. The electrical conductivity increases almost linearly from 0.13 S/cm to 15.7 S/cm with treatment time, while Seebeck coefficient reaches as high as 24.42 $\mu\text{V/K}$ with 30 min treatment time, then decreases to near 20 $\mu\text{V/K}$. Thus, power factor shows an increasing trend with the highest value reaching $661 \times 10^{-3} \mu\text{W/mK}^2$ when treated for 120 min. This demonstrates that the post-treatment of HI vapour could weaken the reduction effect of HI and have positive impact on TE properties of PEDOT:PSS films.

To further study the mechanism for TE properties enhancement, SEM, XPS and Raman spectra studies were conducted. Fig.6(a) shows the thickness of films observed by SEM before and after HI vapour treatment. It appears that the thickness decreases gradually from 100.2 nm to 62.2 nm after 120 min of treatment, which might be attributed to the removing of excessive PSS. Meanwhile, the ratio between PSS and PEDOT calculated by XPS spectra (Fig.6b) shows a decrease from 2.90 to 1.62 after HI vapour treatment, confirming that PSS has been depleted selectively from these films.

As for redox level shown in Fig.6(c), peak enhancement, narrower bands and red shifting are still observed, demonstrating the presence of morphology change and reduction process during HI vapour treatment. Nevertheless, the electrical conductivity is as low as 15.7 S/cm, resulting in a slightly increase in power factor. (150 times higher than that of pristine film)

Compared to HI solution treatment, HI vapour leads to a weak physical doping, which causes a slightly increase in electrical conductivity. Meanwhile, the reduction effect is successfully

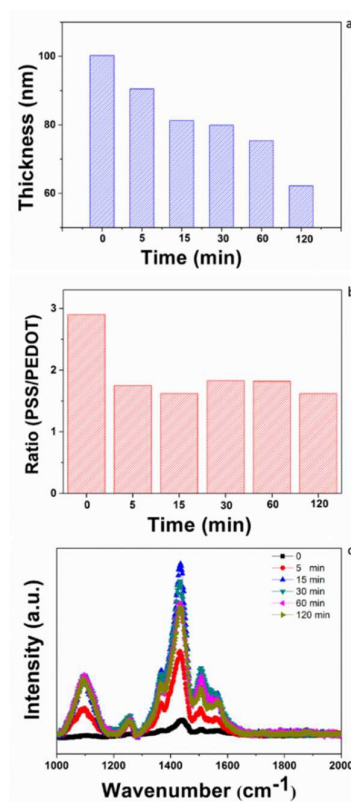


Fig.6 a) Thickness, b) ratios of PSS and PEDOT, c) Raman spectra of nanofilms treated by HI vapour

weakened since the decreasing trend of electrical conductivity is restrained with the extension of time. However, HI vapour is unable to largely deplete PSS, resulting in rather low electrical conductivity and power factor. Thus, strong physical doping and weak reduction effect are needed to further optimize the TE properties of PEDOT:PSS nanofilms

3.3 Two-step treatment via the combination of DMSO and HI vapour

It has been widely reported that high boil-point solvent such as DMSO has important influence on the TE properties of PEDOT:PSS nanofilms^{20, 33}. The excessive PSS can be removed from spin-coated PEDOT:PSS films through DMSO treatment, results in electrical conductivity as high as 952 S/cm. Therefore, to effectively remove PSS before altering the redox level of PEDOT, a two-step treatment via the combination of DMSO and HI vapour is proposed to further improve the TE properties of these nanofilms.

These nanofilms were firstly treated by DMSO for 30 min, then fumigated with HI vapour for different treatment time. Fig.7(a) shows the electrical conductivity decreases (x here is the time treated by HI vapour after DMSO for 30 min, similarly herein after), but still maintains a considerably high level of 298 S/cm after 120 min, while the Seebeck coefficient monotonically increases from 18.98 $\mu\text{V/K}$ to 33.02 $\mu\text{V/K}$ (Fig.7b), which indicates that the presence of reduction during post-treatment process. As a result, the power factor reaches as high as $45.02 \mu\text{W/mK}^2$ after a second step treatment time of 30 min (Fig.7c)

PAPER

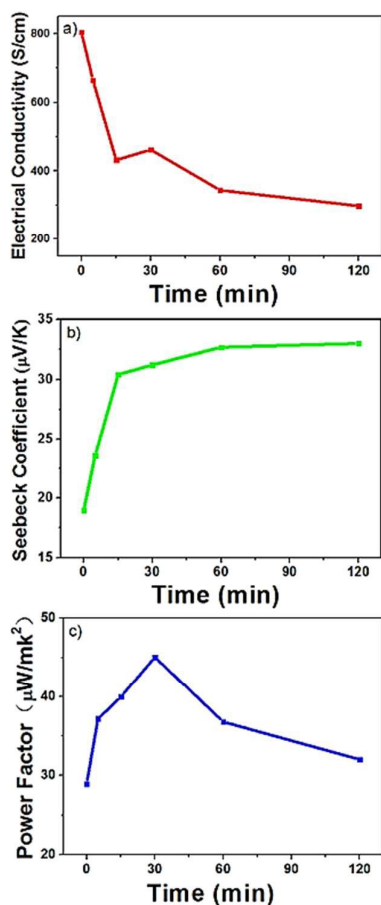


Fig.7 a) electrical conductivity, b) Seebeck coefficient, c) power factor of PEDOT:PSS nanofilms treated by DMSO and HI vapour; as a function of second step treatment time.

Similarly, AFM characterization was used to study the surface morphology of PEDOT:PSS nanofilms. Fig.8 shows the height images and phase images of films before and after treatment by DMSO and HI vapour. Comparing with the pristine film with homogeneous morphology, the grain-like morphology is observed after DMSO treatment, with no apparent change observed after subsequent second step treatment of HI vapour. The roughness of these films shown in Fig.8 are 0.888, 1.678, 1.173, 1.277, 1.537, 1.339, 1.435, respectively. DMSO treated film has the highest roughness among all, which means PSS has been depleted the most by the first step, and the following treatment of HI vapour does not contribute much to the depletion process. Besides, the phase separation becomes blurred when treated by HI vapour, corresponding to the decrease in roughness after treatment by HI vapour. It might be caused by the swelling of samples in the atmosphere of HI vapour.

The thickness comparison (Fig.9a) shows that the thickness of these films decreases dramatically to 43.1 nm when treated by DMSO, indicating that PSS is depleted efficiently by such solvent. After that, the thickness increases when further treated by HI vapour, which is in accordance with the AFM observation where swelling is noted. The thickness of these nanofilms treated by DMSO and HI vapour are lower than those treated by HI vapour only, suggesting that the two-step treatment is much more efficient. Fig.9(b) shows the ratio between PSS and PEDOT. The value decreases sharply from 2.20 to 1.02 when treated by DMSO, then changes not significantly with different second step treatment time. This is in agreement with the results discussed above as the second step treatment has little effect on the PSS content in these nanofilms. Meanwhile, Raman spectra shown in Fig.9(c) indicates HI vapour can effectively reduce these nanofilms and such effect is enhanced with increasing second step treatment time. It is thought that the concentration of charge carrier

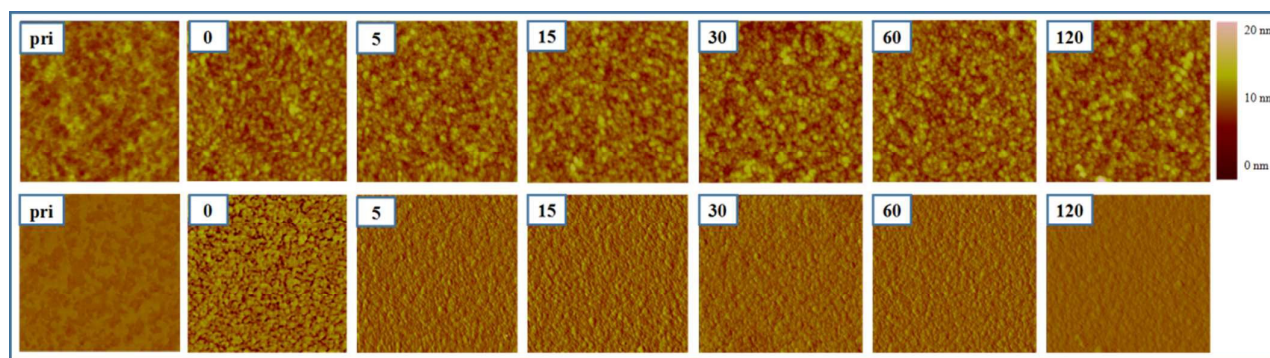


Fig.8 AFM images of pristine PEDOT:PSS nanofilms as well as treated by DMSO and HI vapour with a different second step treatment time (the numbers on the left corner shows treatment time in mins). scanning area: $2 \mu\text{m} \times 2 \mu\text{m}$

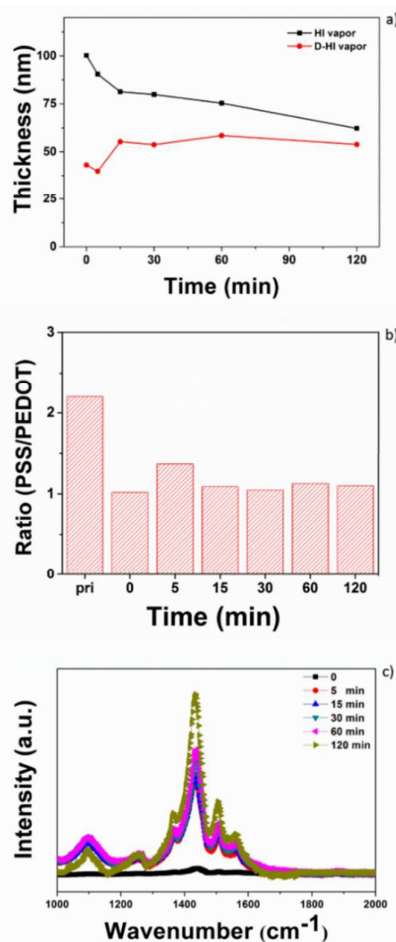


Fig.9 a) Thickness comparison between HI vapour treated films (black square) and DMSO-HI vapour treated films (red spot); b) Ratio between PSS and PEDOT c) Raman spectra for pristine nanofilms as well as nanofilms treated with different second step treatment time.

inside PEDOT:PSS decreases upon reduction, contributing to decreasing electrical conductivity and increasing Seebeck coefficient.

The UV absorption spectra of PEDOT:PSS nanofilms indicates a systematic change of the optical spectra depending on the redox level (Fig.10). It is reported that PEDOT has three redox levels: bipolaron (PEDOT²⁺), polaron (PEDOT⁺) and neutral (PEDOT)^{39, 40}, after reduction process, the redox level of films changes from bipolaron to polaron or neutral, the main peak moves to 900 nm for polaron PEDOT⁺ and to 600 nm for neutral PEDOT. As shown in Fig.10(a) and (c), the peaks decrease dramatically, which is relevant to the electrical conductivity variation. Meanwhile, peaks are

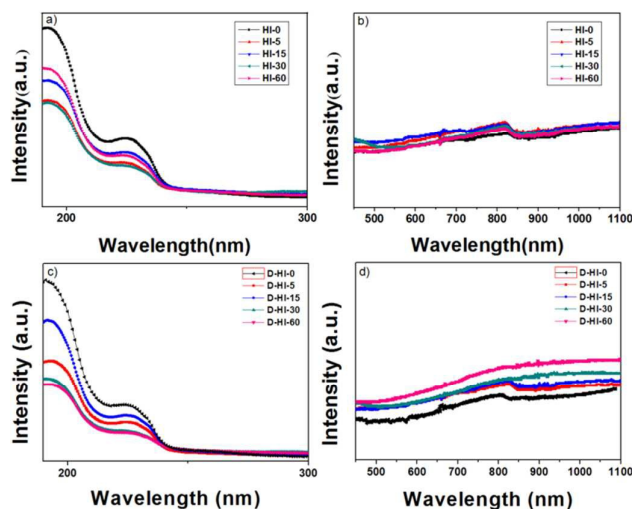
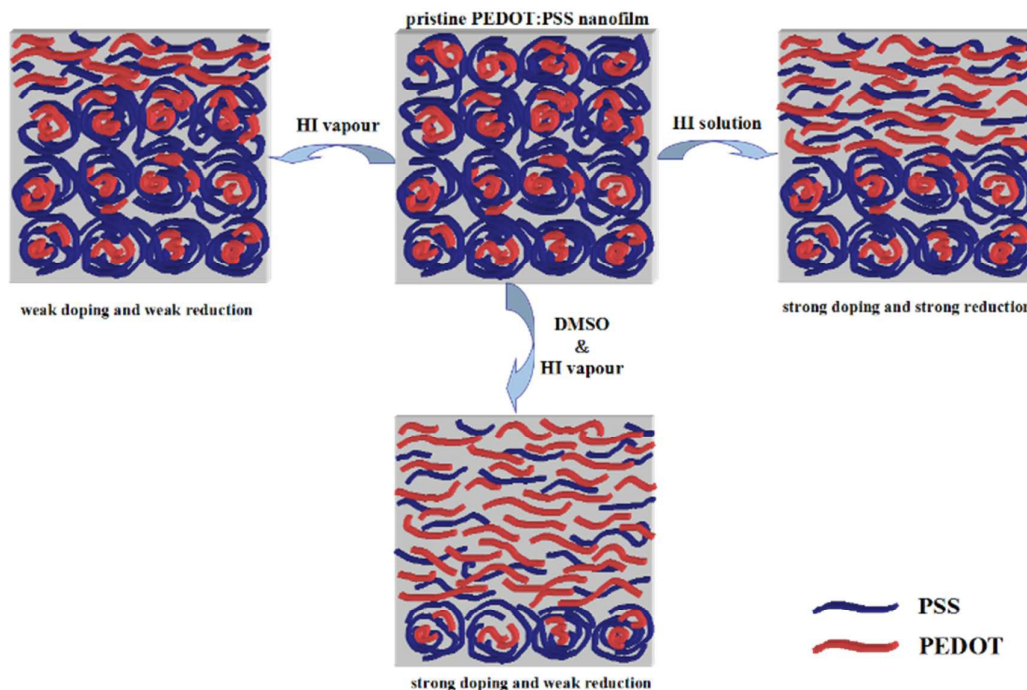


Fig.10 UV absorption spectra of PEDOT:PSS nanofilms: a) wavelength between 190~300 nm for nanofilms treated by HI vapour ;b) wavelength between 450~1100 nm for nanofilms treated by HI vapour ;c) wavelength between 190~300 nm for nanofilms treated by DMSO and HI vapour ;d) wavelength between 450~1100 nm for nanofilms treated by DMSO and HI vapour

observed at about 900 nm in the spectra treated by DMSO and HI vapour in Fig. 10 (d), compared to those treated by HI vapour only as shown in Fig. 10 (b), which might due to that PEDOT was easier to be reduced when exposed to the surface since PSS has been removed by DMSO. No peaks appears at 600 nm indicating the weak reduction effect on PEDOT.

Sketch.1 shows the post-treatment process by three different methods as discussed in this article. HI solution has strong physical doping and reduction effect on PEDOT:PSS films, while HI vapour shows weak physical doping and reduction effect. Compared to treatment using HI solution or HI vapour only, the combination of DMSO and HI vapour treatment is demonstrated to have the most effective influence on TE properties, due to the most depletion of PSS by strong physical doping of DMSO as well as the changing redox level of PEDOT from bipolaron to polaron by weak reduction of HI vapour. Thus, the optimized TE properties of PEDOT:PSS nanofilms was obtained by this novel two-step treatment. The initial electrical conductivity of the untreated PEDOT:PSS films in current study (0.3 S/cm) is considerably lower than some values reported in literature⁴¹ (~600 S/cm). This might be responsible for the lower power factor observed in this study. However, the power factor is quite higher than those inorganic/ polymer based composite films^{42, 43}. Moreover, it is thought that such two-step solvent post-treatment method could offer a novel route to optimize the TE properties of PEDOT:PSS based films.^{42, 44-48}

PAPER



Sketch .1 post-treating process by three different methods

4. Conclusions

In summary, post-treatment of PEDOT:PSS films using HI and DMSO for improved TE properties are studied. Issues including using these solvents in a step-wise fashion, using solvent or vapour and treatment time are considered as important parameters. It is demonstrated that HI has both physical doping and reducing effect on PEDOT:PSS simultaneously, yet, its solution or vapour could not remove most of the excessive PSS to achieve high electrical conductivity. Therefore, DMSO is used to remove PSS first, then, HI vapour was used to alter their redox level. As a result, the power factor reaches as high as $45.02 \mu\text{W}/\text{mK}^2$, which is over 5000 times higher than the as spun film. To gain information on their structural change during post-treatment, these films are characterized with methods including: AFM, XPS, UV, SEM and Raman spectroscopy. It is concluded that the depleting effect of PSS from DMSO and oxidation level change of PEDOT from HI vapour are responsible for the enhanced TE properties. The former leads to enhanced electrical conductivity and the later leads to reduced charge carrier concentration, thus, enhanced Seebeck coefficient. Such two-solvent post-treatment method could provide a novel route to optimize the TE properties of PEDOT:PSS based film

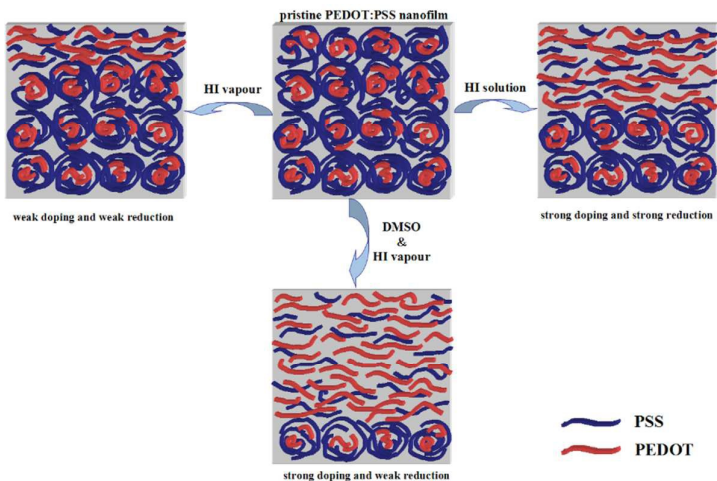
Acknowledgements

We express our sincere thanks to the National Natural Science Foundation of China for financial support (51273117 and 51421061). H. Deng would like to thank the Ministry of Education (Program for

New Century Excellent Talents in University, NCET-13-0383), the Innovation Team Program of Science & Technology Department of Sichuan Province (2014TD0002) and Sichuan Province for financial support (2013JQ0008). We also would like to thank Dr. Emiliano Bilotti from Queen Mary, University of London, UK and Mr. Yichun Wu from Namicro, GIANT (Wuhan China) for carrying out calibration experiment for current thermoelectric measurement system.

Notes and references

1. P. J. Taroni, I. Hoces, N. Stingelin, M. Heeney and E. Bilotti, *Isr. J. Chem.*, 2014, **54**, 534-552.
2. T. Dittrich, A. Belaidi and A. Ennaoui, *Sol. Energy Mater. Sol. Cells*, 2011, **95**, 1527-1536.
3. Q. Zhang, Y. Sun, W. Xu and D. Zhu, *Adv. Mater.*, 2014, **26**, 6829-6851.
4. G. J. Snyder and E. S. Toberer, *Nat. Mater.*, 2008, **7**, 105-114.
5. M. Vosgueritchian, D. J. Lipomi and Z. Bao, *Adv. Funct. Mater.*, 2012, **22**, 421-428.
6. R. Yue and J. Xu, *Synthetic Met.*, 2012, **162**, 912-917.
7. N. Dubey and M. Leclerc, *J. Polym. Sci., Part B: Polym. Phys.*, 2011, **49**, 467-475.
8. D. Maddison, J. Unsworth and R. Roberts, *Synthetic Met.*, 1988, **26**, 99-108.
9. B. Zhang, J. Sun, H. Katz, F. Fang and R. Opila, *ACS Appl. Mater. Interfaces*, 2010, **2**, 3170-3178.
10. H. Yan, T. Ohta and N. Toshima, *Macromol. Mater. Eng.*, 2001, **286**, 139-142.
11. F. Yakuphanoglu and B. Senkal, *J. Mater. Chem. C*, 2007, **111**, 1840-1846.
12. R. B. Aïch, N. Blouin, A. Bouchard and M. Leclerc, *Chem. Mater.*, 2009, **21**, 751-757.
13. Y. Shinohara, K. Ohara, H. Nakanishi, Y. Imai and Y. Isoda, 2005.
14. J. Sun, M.-L. Yeh, B. Jung, B. Zhang, J. Feser, A. Majumdar and H. Katz, *Macromolecules*, 2010, **43**, 2897-2903.
15. L. Bao-Yang, L. Cong-Cong, L. Shan, X. Jing-Kun, J. Feng-Xing, L. Yu-Zhen and Z. Zhuo, *Chin. Phys. Lett.*, 2010, **27**, 057201.
16. M. Culebras, S. Gómez and A. Cantarero, *J. Mater. Chem. A*, 2014, **2**, 10109-10115.
17. O. Bubnova, Z. U. Khan, A. Malti, S. Braun, M. Fahlman, M. Berggren and X. Crispin, *Nat. Mater.*, 2011, **10**, 429-433.
18. S. Jönsson, J. Birgersson, X. Crispin, G. Greczynski, W. Osikowicz, A. D. Van Der Gon, W. R. Salaneck and M. Fahlman, *Synthetic Met.*, 2003, **139**, 1-10.
19. X. Crispin, F. Jakobsson, A. Crispin, P. Grim, P. Andersson, A. Volodin, C. Van Haesendonck, M. Van der Auweraer, W. R. Salaneck and M. Berggren, *Chem. Mater.*, 2006, **18**, 4354-4360.
20. H. Park, S. H. Lee, F. S. Kim, H. H. Choi, I. W. Cheong and J. H. Kim, *J. Mater. Chem. A*, 2014, **2**, 6532-6539.
21. P. Kumar, K. Santhakumar, J. Tatsugi, P.-K. Shin and S. Ochiai, *Jpn. J. Appl. Phys.*, 2014, **53**, 01AB08.
22. Y. H. Kim, C. Sachse, M. L. Machala, C. May, L. Müller - Meskamp and K. Leo, *Adv. Funct. Mater.*, 2011, **21**, 1076-1081.
23. O. Bubnova, M. Berggren and X. Crispin, *J. Am. Chem. Soc.*, 2012, **134**, 16456-16459.
24. T.-C. Tsai, H.-C. Chang, C.-H. Chen and W.-T. Whang, *Org. Electron.*, 2011, **12**, 2159-2164.
25. Q. Wei, M. Mukaida, Y. Naitoh and T. Ishida, *Adv. Mater.*, 2013, **25**, 2831-2836.
26. C. Liu, B. Lu, J. Yan, J. Xu, R. Yue, Z. Zhu, S. Zhou, X. Hu, Z. Zhang and P. Chen, *Synthetic Met.*, 2010, **160**, 2481-2485.
27. S. Pei, J. Zhao, J. Du, W. Ren and H.-M. Cheng, *Carbon*, 2010, **48**, 4466-4474.
28. Y. Xia, K. Sun and J. Ouyang, *Adv. Mater.*, 2012, **24**, 2436-2440.
29. A. K. Sarker, J. Kim, B.-H. Wee, H.-J. Song, Y. Lee, J.-D. Hong and C. Lee, *RSC Adv.*, 2015, **5**, 52019-52025.
30. X. Wu, J. Liu and G. He, *Org. Electron.*, 2015, **22**, 160-165.
31. D. A. Mengistie, C.-H. Chen, K. M. Boopathi, F. W. Pranoto, L.-J. Li and C.-W. Chu, *ACS Appl. Mater. Interfaces*, 2014, **7**, 94-100.
32. N. Massonnet, A. Carella, O. Jaudouin, P. Rannou, G. Laval, C. Celle and J.-P. Simonato, *J. Mater. Chem. C*, 2014, **2**, 1278-1283.
33. S. Liu, H. Deng, Y. Zhao, S. Ren and Q. Fu, *RSC Adv.*, 2015, **5**, 1910-1917.
34. G. Zotti, S. Zecchin, G. Schiavon, F. Louwet, L. Groenendaal, X. Crispin, W. Osikowicz, W. Salaneck and M. Fahlman, *Macromolecules*, 2003, **36**, 3337-3344.
35. G. Greczynski, T. Kugler and W. Salaneck, *Thin Solid Films*, 1999, **354**, 129-135.
36. J. P. Thomas, L. Zhao, D. McGillivray and K. T. Leung, *J. Mater. Chem. A*, 2014, **2**, 2383-2389.
37. V. Singh, S. Arora, M. Arora, V. Sharma and R. Tandon, *Semicond. Sci. Technol.*, 2014, **29**, 045020.
38. M. De Kok, M. Buechel, S. Vulto, P. Van de Weijer, E. Meulenkaamp, S. De Winter, A. Mank, H. Vorstenbosch, C. Weijtens and V. Van Elsbergen, *physica status solidi (a)*, 2004, **201**, 1342-1359.
39. S. H. Lee, H. Park, S. Kim, W. Son, I. W. Cheong and J. H. Kim, *J. Mater. Chem. A*, 2014, **2**, 7288-7294.
40. J. Luo, D. Billep, T. Waechtler, T. Otto, M. Toader, O. Gordan, E. Sheremet, J. Martin, M. Hietschold and D. R. Zahn, *J. Mater. Chem. A*, 2013, **1**, 7576-7583.
41. G. Kim, L. Shao, K. Zhang and K. P. Pipe, *Nat. Mater.*, 2013, **12**, 719-723.
42. Y. Du, K. Cai, S. Chen, P. Cizek and T. Lin, *ACS Appl. Mater. Interfaces*, 2014, **6**, 5735-5743.
43. H. Song, C. Liu, H. Zhu, F. Kong, B. Lu, J. Xu, J. Wang and F. Zhao, *J. Electron. Mater.*, 2013, **42**, 1268-1274.
44. Y. Du, S. Z. Shen, K. Cai and P. S. Casey, *Prog. Polym. Sci.*, 2012, **37**, 820-841.
45. J. Zhou and G. Lubineau, *ACS Appl. Mater. Interfaces*, 2013, **5**, 6189-6200.
46. J. Grunlan, C. Yu, Y. S. Kim, K. Choi and D. Kim, 2010.
47. D. Kim, Y. Kim, K. Choi, J. C. Grunlan and C. Yu, *ACS Nano*, 2009, **4**, 513-523.
48. C. Yu, K. Choi, L. Yin and J. C. Grunlan, *ACS nano*, 2011, **5**, 7885-7892.



Large enhancement of TE properties via a novel two-step post treatment